J. Membrane Biol. 192, 191–201 (2003)
DOI: 10.1007/s00232-002-1075-8

The Journal of
Membrane
Biology

A Hypertonicity-activated Nonselective Conductance in Single Proximal Tubule Cells Isolated from Mouse Kidney

K.J.D. Balloch, J.A. Hartley, I.D. Millar, J.D. Kibble[1], L. Robson
Department of Biomedical Science, Western Bank, University of Sheffield, Sheffield, S10 2TN, UK and [1]Department of Physiology and Neuroscience, St. George's University, True Blue Campus, P.O. Box 7, St. George's, GRENADA, W.I.

Received: 15 August 2002/Revised: 24 December 2002

Abstract. The whole-cell patch-clamp technique was used to examine nonselective conductances in single proximal tubule cells isolated from mouse kidney. Single cells were isolated in either the presence or absence of a cocktail designed to stimulate cAMP. Patches were obtained with Na^+ Ringer in the bath and Cs^+ Ringer in the pipette. On initially achieving the whole-cell configuration, whole-cell currents were small. In cAMP-stimulated cells, with 5 mM ATP in the pipette solution, whole-cell currents increased with time. The activated current was linear, slightly cation-selective, did not discriminate between Na^+ and K^+ and was inhibited by 100 μM gadolinium. These properties are consistent with the activation of a nonselective conductance, designated G_{NS}. Activation of G_{NS} was abolished with pipette AMP-PNP, ATP plus alkaline phosphatase or in the absence of ATP. In unstimulated cells G_{NS} was activated by pipette ATP together with PKA. These data support the hypothesis that G_{NS} is activated by a PKA-mediated phosphorylation event. G_{NS} was also activated by a hypertonic shock. However, G_{NS} does not appear to be involved in regulatory volume increase (RVI), as RVI was unaffected in the presence of the G_{NS} blocker gadolinium. Instead, the ATP sensitivity of G_{NS} suggests that it may be regulated by the metabolic state of the renal proximal tubule cell.

Key words: Renal proximal tubule — Nonselective conductance — PKA — Hypertonic — RVI — ATP

Introduction

Most cells are capable of regulating their volume in response to anisotonic media (Waldegger et al., 1998). Regulatory volume decrease (RVD) is observed in response to cell swelling. RVD acts to bring cell volume back to normal and occurs as a consequence of the loss of osmotically active solutes from the cell such as K^+, Cl^- and HCO_3^- via both conductive and cotransport pathways (Lopes & Guggino, 1987; Welling & O'Neil, 1990). Cell shrinkage is associated with regulatory volume increase (RVI). RVI acts to bring cell volume back up to normal and occurs as a consequence of the activation of solute influx pathways for Na^+ and Cl^-. A number of different cotransporters and counter-transporters mediate this uptake of Na^+ and Cl^-. In particular there is evidence for a role for the bumetanide-sensitive Na^+-K^+-$2Cl^-$ cotransporter, the Na^+-H^+ exchanger and the Cl^--HCO_3^- exchanger (Douglas & Brown, 1996; Wehner & Tinel, 1998; Miley et al., 1998).

In addition to these channels and transporters it has also been suggested that nonselective cation channels may play an important role in cell volume regulation. Nonselective cation channels are ubiquitously expressed in a wide range of cells types (Sachs, 1987; Wison, Magoski & Kaczmarek, 1998; Takenaka et al., 1998). They can be subdivided into two basic groups, those that are activated by an increase in cell volume and those activated by cell shrinkage. The swelling-activated cation channels are thought to play an important role in RVD. They are typically Ca^{2+} permeable and on activation are thought to lead to a rise in intracellular Ca^{2+} and subsequent activation of solute exit pathways. They have been observed in a number of different cells, including the renal proximal tubule (Christensen, 1987; Gustin et al., 1988; Bear, 1990; Filipovic & Sackin, 1991; Wellner & Isenberg, 1993; Hurwitz, Hu & Segal, 2002). The shrinkage-activated cation channels have only been identified in a small number of cells. These include the mouse and rat collecting ducts, human colonic carcinoma cells, a renal proximal tubule cell line, smooth muscle cells, neuroblastoma cells and human airway cells (Chan &

Correspondence to: L. Robson; email: l.robson@sheffield.ac.uk

Nelson, 1992; Volk, Frömter & Korbmacher, 1995; Schlatter et al., 1997; Koch & Korbmacher, 1999). Physiologically, these hypertonic-activated channels are thought to mediate Na^+ uptake in RVI. Although evidence supporting this hypothesis has only been demonstrated in a human hepatoma cell line HepG2 (Wehner, Lawonn & Tinel, 2002). In that study, inhibitors of a hypertonic-activated cation conductance also inhibited RVI. The following study describes a hypertonic shock-activated conductance in mouse renal proximal tubule cells, designated G_{NS}, and investigates the role of G_{NS} in RVI.

Materials and Methods

Cell Isolation

Single proximal tubule cells were isolated from mouse kidney using a variation of a technique described previously (Hoyer & Goegelein, 1991). MF1 Albino Swiss or C57/black6 mice were killed humanely by concussion followed by cervical dislocation. Kidneys were removed and placed in a beaker containing ice-cold isolation buffer, which contained (in mM): 140 KCl, 1 $MgCl_2$, 1 $CaCl_2$ and 10 HEPES (titrated to pH 7.4 with KOH). To activate cAMP-dependent conductances, this Ringer also contained 2 μM forskolin, 100 μM dibutyryl cAMP (dbcAMP) and 100 μM 3-isobutyl-1-methylxanthine (IBMX). This Ringer was oxygenated for fifteen minutes before use. In some experiments, cells were not stimulated with the cAMP cocktail, and were isolated with the standard isolation Ringer in the absence of forskolin, dbcAMP and IBMX. The membranous kidney capsule was removed and the kidney longitudinally bisected. Tangential slices of cortex were cut off and placed into a few drops of isolation buffer in a small glass petri dish. The tissue slices were then diced between two single edged razors and 2 to 3 ml of isolation buffer added to the tissue fragments. This suspension was transferred to a glass/Teflon homogenizer. Two strokes of the homogenizer pestle were applied and the resulting suspension filtered through a nylon mesh (PP80, Millipore, Ireland). The cell suspension was then stored in the isolation Ringer under ice. The entire procedure was performed over ice using prechilled glassware. Cells prepared in this manner were spherical and did not display any obvious brush-border morphology under light microscopy. Proximal tubule cells were identified from the cortex preparation by size (*see* cell diameter experiments).

Patch-Clamp Experiments

A suspension of single MF1 cells was placed in a Perspex bath on the stage of an inverted microscope (Olympus IX70) and whole-cell patch-clamp techniques employed to investigate whole-cell currents (Hamill et al., 1981). Voltage protocols were driven from an IBM-compatible computer equipped with a Digidata interface (Axon Instruments, Foster City, CA), using the pClamp software, Clampex (Axon Instruments). Recordings were made using a List EPC-7 amplifier (Heka, Germany). Patches were initially held at a potential of −40 mV and then stepped to between +40 and −100 mV in −20 mV steps. Whole-cell currents were saved directly onto the hard disk of the computer following low-pass filtering at 5 kHz. Average steady-state currents at each potential were derived using Microsoft Excel 2000. The reversal potentials (V_{rev}) of ohmic and rectifying currents were calculated by linear or polynomial regression, respectively. In patch-clamp experiments, unless otherwise specified, the pipette solution was a low-Ca^{2+} Ringer, which contained (in mM): 140 CsCl, 2 $MgCl_2$, 0.5 EGTA, 5 MgATP and 10 HEPES (titrated to pH 7.4 with CsOH). Cs^+ in the pipette inhibited K^+ conductances. In patch-clamp experiments, unless otherwise specified, the bath solution was a high-Ca^{2+} Ringer, which contained (in mM): 115 NaCl, 2 $CaCl_2$, 1 $MgCl_2$, 50 mannitol and 10 HEPES (titrated to pH 7.4 with NaOH).

Patch-Clamp Protocols

In all experiments, whole-cell currents were recorded initially on achieving the whole-cell configuration and again at steady state between 4 and 14 minutes after achieving the whole-cell configuration. The only exception to this were experiments using unstimulated cells investigating the effect of protein kinase A in the pipette, where steady state was achieved by 25 minutes. To discriminate between patches demonstrating current activation versus a change in leak conductance, patches were only used for analysis when the increase in cell current was sensitive to inhibition by Gd^{3+} and/or the increase in current reached a new stable level.

Role of Intracellular ATP

To examine the effect of intracellular ATP, initial and steady-state whole-cell currents were recorded in the presence of 5 mM pipette ATP or in the absence of pipette ATP (addition of mannitol).

Sensitivity to Gadolinium (Gd^{3+})

On achieving steady-state, 100 μM Gd^{3+} was added to the bath to examine the sensitivity of whole-cell currents. Gd^{3+} was subsequently washed from the bath to examine the reversibility of any inhibition. To examine the dose response to Gd^{3+}, concentrations between 0.1 and 300 μM were added to the bath after achieving steady state.

Cation:Anion Selectivity

The cation-to-anion selectivity of total whole-cell current was examined initially on achieving the whole-cell configuration and again at steady state using a dilution protocol. Bath NaCl was decreased fivefold from 115 mM to 23 mM (addition of mannitol to maintain osmolality). Under this circumstance the V_{rev} of cation-selective currents shifts in a negative direction, while the V_{rev} of anion-selective currents shifts in a positive direction. Therefore, by recording the shift in V_{rev} experimentally, the cation-to-anion selectivity of currents can be determined. The cation-to-anion selectivity of the Gd^{3+}-sensitive currents was determined in unpaired cells due to the irreversible blocking action of this cation (*see* Results). Values were corrected for the junction-potential change that occurs on dropping bath NaCl fivefold. The junction-potential change was measured using a flowing 3 M KCl reference electrode. To determine the Na^+:K^+ selectivity of steady-state currents, 115 mM bath Na^+ was replaced by 115 mM K^+. The *N*-methyl D-glucosamine (NMDG) : Na^+ selectivity of Gd^{3+}-sensitive currents was determined from the shift in V_{rev} of Gd^{3+}-sensitive currents observed when bath NaCl (115 mM) was substituted by 115 mM NMDG-Cl. These experiments were carried out in unpaired cells due to the irreversible blocking action of Gd^{3+} (*see* Results).

Role of Phosphorylation

Initial and steady-state whole-cell currents were examined in cAMP-prestimulated cells with 5 mM ATP plus 25 units per ml of

alkaline phosphatase in the pipette. If the activation of currents by ATP requires phosphorylation, then alkaline phosphatase would be expected to inhibit activation. In addition, initial and steady-state whole-cell currents were examined with 5 mM 5′-adenylimidodiphosphate (AMP-PNP) in the pipette, a non-hydrolyzable analogue of ATP. In the unstimulated cells, initial currents and steady-state currents measured at 25 minutes were examined with 5 mM ATP plus 375 nM protein kinase A (PKA) catalytic subunit. The Gd^{3+}-sensitivity of the PKA-activated currents was determined by the addition of 100 μM Gd^{3+} to the bath at 25 minutes.

Regulation by Hypertonic Shock

The effect of an osmotic shock on steady-state currents was examined by the addition of 40 mM mannitol to the bath.

Cell diameter protocols

The diameter of cells was measured with either a photodiode array-based system as described previously (Robson & Hunter, 1994) or a digital camera-based system (SoftEdge, IonOptix, MA). To identify the proximal cells in the mixed cell population isolated in the C57B mouse kidney cortex preparation, the response of all cells to addition of 10 mM L-alanine was examined. An increase in cell diameter in response to L-alanine was taken as an indicator of proximal tubule function. Cells were initially superfused with mammalian Ringer, which contained (mM): 112 NaCl, 5 KCl, 2 $CaCl_2$, 1 $MgCl_2$, 60 mannitol and 10 HEPES titrated to pH 7.4 with NaOH and then 10 mM L-alanine added to the bath. When 10 mM L-alanine was added to the bath mannitol was removed to maintain osmolality.

To examine the effect of a hypertonic shock, both unstimulated and cAMP-prestimulated cells were initially supervised with a control Ringer, which contained (in mM): 115 NaCl, 5 KCl, 2 $CaCl_2$, 1 $MgCl_2$, 10 HEPES (titrated to pH 7.4 with NaOH) and 40 mannitol. Once a constant cell diameter was achieved, the bath solution was exchanged for one to which an additional 40 mM mannitol was added to provide the hypertonic stimulus. Cells were then allowed a period of at least 10 min to recover their original diameter, i.e., undergo RVI, and achieve a steady-state diameter before being returned to control Ringer. To investigate the effects of Gd^{3+} on RVI, cell diameter experiments were performed on cAMP prestimulated cells in the presence of 100 μM Gd^{3+}. Gd^{3+} was added to both the control and hypertonic bath solutions. A final series of experiments investigated the cell diameter responses to hypertonicity in cAMP-prestimulated cells prepared in the presence of 100 μM Gd^{3+} in the cell isolation buffer.

Solutions

The osmolality of all solutions was measured (Roebling osmometer) and adjusted to within 1 mosmol·kg^{-1}·H_2O of 300 mosmol·kg^{-1}·H_2O with water or mannitol, as appropriate. All chemicals were obtained from Sigma or Calbiochem, and were of analytical grade.

Statistics

All data are given as mean ± SEM. Statistical significance was determined using Student's *t*-test, one-sample *t*-test, ANOVA or Fisher's Exact Probability Test, as appropriate, and significance was assumed at the 5% level.

Results

Identification of Renal Proximal Tubule Cells

The initial diameter of cells was 9.39 ± 0.12 μm (n = 19). On the addition of L-alanine, cell diameter increased by 0.26 ± 0.02 μm to 9.65 ± 0.12 μm. On removal of L-alanine, cell diameter recovered to 9.31 ± 0.15 μm. The size range of cells that responded to L-alanine was 8.75 μm to 10.5 μm and all cells tested within this size range responded to L-alanine. Cells falling within this range were therefore taken as proximal tubule cells.

Identification of a Nonselective Conductance

In the prestimulated cells in the presence of 5 mM pipette ATP, the initial whole-cell currents were relatively small (Fig. 1). However, the magnitude of these currents increased over time. The steady-state current was defined as the current level that was maintained in two subsequent voltage protocols and was observed at 9.11 ± 1.28 minutes (n = 9, Fig. 1). The total currents recorded either initially or at steady state were ohmic over the voltage range investigated and could be fitted with a linear regression, r^2 = 0.99, for both the initial and steady-state currents. In conjunction with the increase in current magnitude, the cation selectivity of the whole-cell currents increased. The initial V_{rev} of currents with 115 NaCl in the bath was −1.96 ± 1.05 mV (n = 7). Dilution of bath NaCl to 23 mM was not associated with a change in V_{rev}, which was maintained at −6.34 ± 3.13 mV. However, after the increase in current magnitude had reached steady state a significant shift in V_{rev} was observed. In 115 mM NaCl, the V_{rev} of whole cell currents was −2.17 ± 0.59 mV (n = 7). This shifted in a negative direction to −10.4 ± 0.65 mV on dilution of bath NaCl to 23 mM, a mean shift of −8.18 ± 0.55 mV. This corresponds to a cation:anion selectivity ratio of 1.48 ± 0.04, which was significantly greater than unity. Substitution of bath Na^+ for K^+ did not give a significant shift in V_{rev}, −2.1 ± 1.1 mV (n = 6), corresponding to a Na^+:K^+ selectivity ratio of 0.9 ± 0.2.

The activated current was inhibited by Gd^{3+} (Fig. 2). Addition of Gd^{3+} to the bath decreased the currents recorded at all potentials. On removal of Gd^{3+} from the bath there was no significant current recovery, and currents remained below the steady-state level, Fig. 2*C*. The Gd^{3+}-sensitive currents were cation selective. The V_{rev} of the Gd^{3+}-sensitive currents in 115 mM NaCl was −2.98 ± 0.71 mV (n = 7, Fig. 3). This shifted, in unpaired cells, to −18.0 ± 2.63 mV (n = 9) on dilution of NaCl to 23 mM, corresponding to a cation:anion selectivity ratio of 2.11 (Fig. 3). In the NMDG:Na^+ selectivity

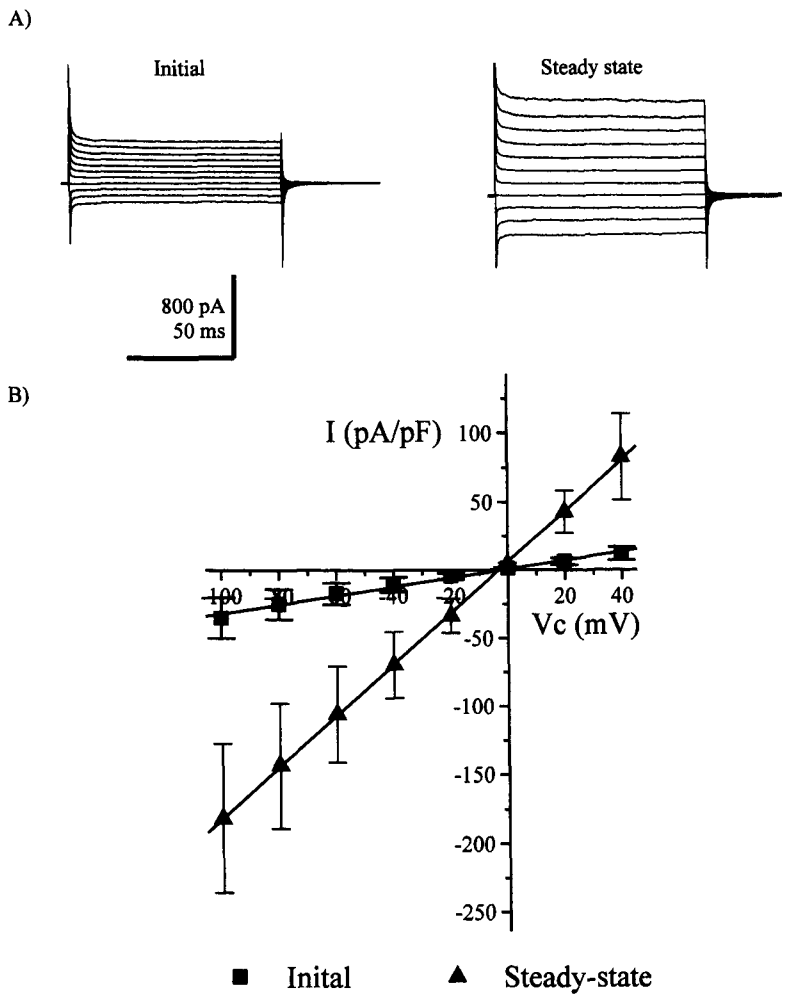

Fig. 1. Spontaneous activation of whole-cell currents recorded from cAMP prestimulated cells in the presence of 5 mM pipette ATP. (*A*) Typical traces recorded from the same cell on initially achieving the whole-cell configuration and at steady state. (*B*) Mean whole-cell currents, normalized with respect to capacitance, obtained from 9 prestimulated cells in the presence of 5 mM pipette ATP. The lines through the points are the best fit to a linear regression.

experiments, the V_{rev} of the Gd^{3+}-sensitive current in 115 NaCl was 2.69 ± 1.15 mV (n = 10). The V_{rev} of the Gd^{3+}-sensitive current in 115 NMDG-Cl was −5.01 ± 3.80 mV (n = 7). This gave a NMDG: Na^+ selectivity ratio of 0.74. Interestingly, the magnitude of both the outward and inward Gd^{3+}-sensitive currents were significantly smaller with NMGD as the bath cation compared to Na^+. At +40 mV the Gd^{3+}-sensitive current was 66.4 ± 17.4 pA/pF (n = 10) versus 12.1 ± 4.43 pA/pF (n = 7) in NaCl and NMDG-Cl respectively. At −40 mV the Gd^{3+}-sensitive current was −67.7 ± 16.7 pA/pF (n = 10) versus −16.3 ± 5.93 pA/pF (n = 7) in NaCl and NMDG-Cl respectively. Dose response studies demonstrated that maximal inhibition by Gd^{3+} was achieved with 300 μM. The K_d for inhibition by Gd^{3+} at −80 mV was 75.2 ± 10.4 μM, with a Hill coefficient of 2.4 ± 0.52 (n = 7, r^2 = 0.99 ± 0.01).

Mechanism of Activation of G_{NS}

The activation of whole-cell currents in prestimulated cells was examined under a number of different conditions, in the absence of ATP (substitution by mannitol to maintain osmolality), in the presence of 5 mM AMP-PNP or with 5 mM ATP plus alkaline phosphatase in the pipette. In addition, whole-cell current activation was examined in control cells that were not prestimulated. In these cells the pipette contained either 5 mM ATP or 5 mM ATP plus 375 nM PKA.

The initial currents recorded on achieving the whole-cell configuration were not significantly different between the experimental groups, the ANOVA F value at +40 mV was $F_{5,39}$ = 0.86 and $F_{5,39}$ = 0.87 at −40 mV. In the prestimulated cells current activation was completely inhibited in the absence of pipette ATP and in the presence of either 5 mM AMP-PNP or 5 mM ATP plus alkaline phosphatase (Fig. 4). In unstimulated cells current activation was absent with 5 mM ATP in the pipette. However, activation was observed when the 5 mM ATP pipette solution was supplemented with PKA, although this was attenuated compared to the activation observed in the prestimulated cells with 5 mM ATP (Fig. 4). Of the ten cells examined using PKA, three showed no response and were omitted from the dataset. Like the current activated in the

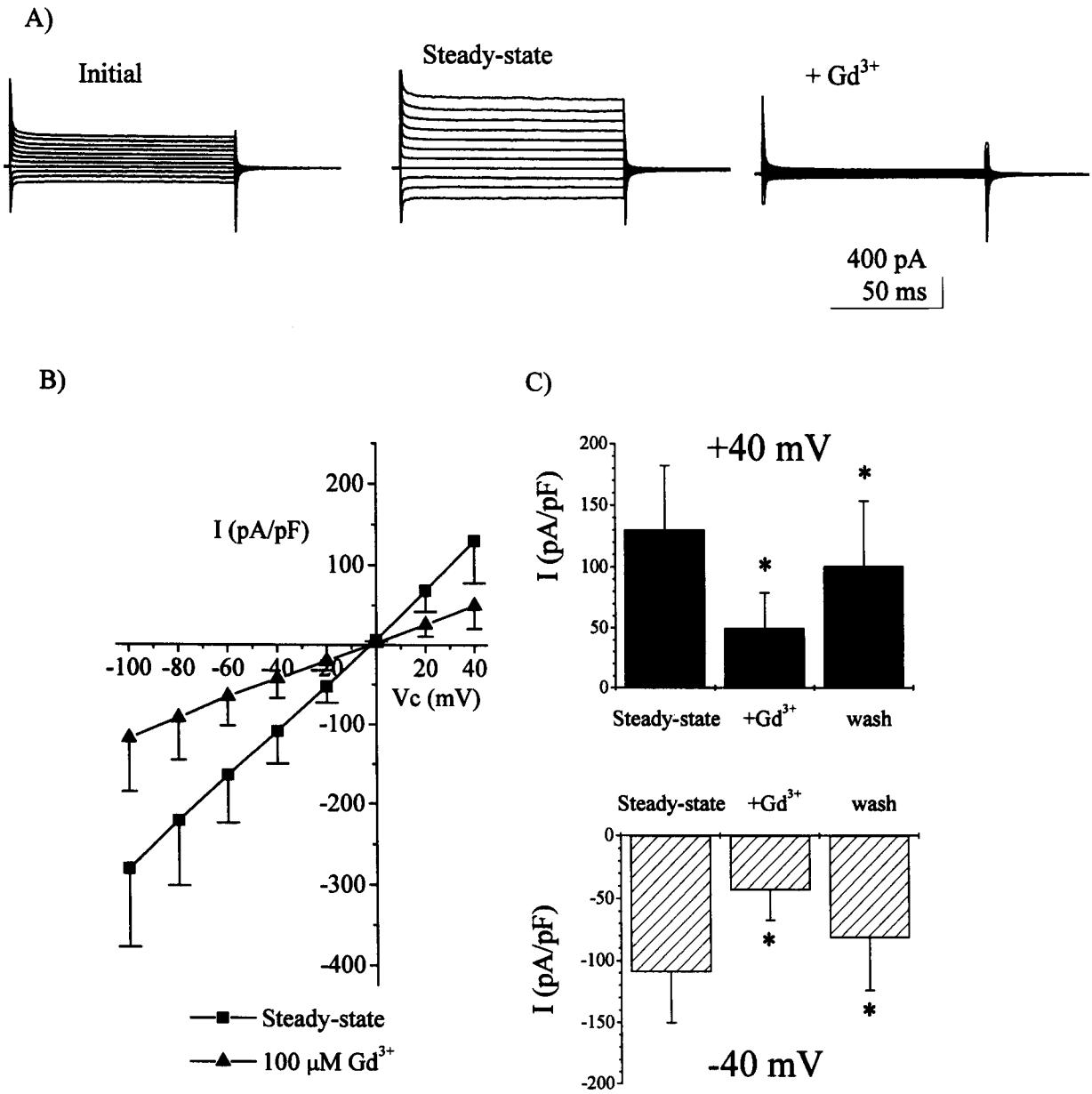

Fig. 2. Effect of Gd^{3+} on steady-state currents activated by cAMP prestimulation and 5 mM pipette ATP. (*A*) Typical current traces recorded from the same cell initially, at steady state and at steady state in the presence of 100 μM Gd^{3+}. (*B*) Mean data showing the effect of Gd^{3+} on 7 cells. (*C*) Mean data showing the partial recovery from Gd^{3+} at +40 mV (*upper panel*) and −40 mV (*lower panel*) (n = 7).

prestimulated cells with 5 mM ATP in the pipette, the PKA-activated current was also sensitive to Gd^{3+}. At +40 mV, 100 μM Gd^{3+} reduced whole-cell current from 25.7 ± 9.00 pA/pF to 17.7 ± 9.68 pA/pF (n = 6). At −40 mV, Gd^{3+} reduced whole cell current from −23.4 ± 8.44 pA/pF to −14.4 ± 7.62 pA/pF (n = 6). The activated current also increased the cation selectivity of the cell. Initially, dilution of bath NaCl did not give a significant shift in V_{rev}, −1.68 ± 3.06 mV (n = 5). However, at steady-state, dilution of NaCl gave a significant shift in V_{rev}, −5.66 ± 0.97 mV (n = 5) corresponding to a cation :anion selectivity ratio of 1.35 ± 0.06 (n = 5).

Effect of Hypertonic Shock

The effect of hypertonic shock on whole-cell currents was investigated in the prestimulated and unstimulated cells with 5 mM ATP in the pipette. Whole-cell clamp was obtained, and currents recorded initially and then at steady state. Once steady state was achieved, cells were exposed to a hypertonic shock (addition of 40 mM mannitol). In the cAMP-prestimulated cells, whole-cell currents increased on exposure to hypertonic Ringer (Fig. 5, n = 10). These currents were inhibited by the addition of 100 μM Gd^{3+} to the bath (Fig. 5). In the unstimulated cells hypertonic shock did not give a significant current

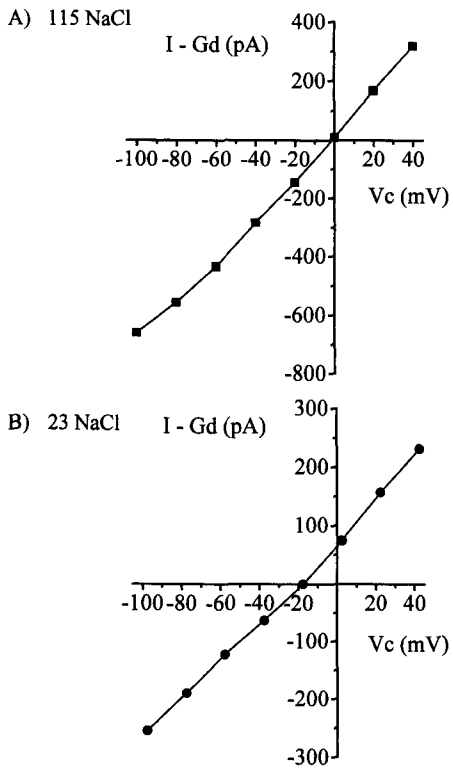

Fig. 3. Cation:anion selectivity of the Gd^{3+}-sensitive current. (*A*) Current recorded from a single cell with 115 mM NaCl in the bath. (*B*) Current recorded from a single cell with 23 mM NaCl in the bath.

activation (Fig. 5, $n = 7$). However, there was no significant difference between the currents measured in the hypertonic Ringer of stimulated and nonstimulated cells when these were expressed as a fraction of the initial current level (*data not shown*).

Cell Diameter

Upon exposure to a 40 mosM hypertonic shock there was an initial decrease of cell diameter followed by two types of response: (1) RVI where the cell diameter increased back towards control values and (2) maintenance of cell diameter for at least ten minutes with recovery only initiated when cells were placed back in the control Ringer (Fig. 6). Cells demonstrating these responses were labelled regulating and nonregulating cells, respectively.

In the unstimulated cells, 7 of 16 (44%) cells demonstrated RVI. The initial diameter of the regulating cells was 10.2 ± 0.19 μm ($n = 7$). This decreased to 9.81 ± 0.18 μm on exposure to the hypertonic Ringer, before recovery to 10.25 ± 0.18 μm after RVI. Placing the regulating cells back in control Ringer increased cell diameter to 10.5 ± 0.21 μm. The initial diameter of the nonregulating cells was 9.56 ± 0.27 μm ($n = 9$). This decreased to 8.95 ± 0.28 μm on exposure to the hypertonic Ringer. No diameter recovery was observed. On placing the nonregulating cells in control Ringer, cell diameter recovered to 9.17 ± 0.28 μm.

With cAMP prestimulation, 7 of 12 (58%) cells demonstrated RVI. In the presence of 100 μM Gd^{3+}, 6 of 13 (46%) cells demonstrated RVI, while 9 of 13 (69%) cells isolated in the presence of Gd^{3+} demonstrated RVI. There was no significant difference between the proportion of cells demonstrating RVI between the groups. In addition, in the regulating cells, neither cAMP prestimulation nor Gd^{3+} had an effect on either the magnitude of shrinkage observed with the hypertonic shock (regulating cells maximum-decrease data ANOVA F value $F_{3,25} = 0.38$) or on RVI (regulating cells difference data, ANOVA F value $F_{3,25} = 1.50$), Table 1. In the nonregulating cells the maximum decrease in cell diameter of the unstimulated cells was significantly greater than the decrease observed with cAMP prestimulation or Gd^{3+} (nonregulating cells maximum decrease, ANOVA F value $F_{3,21} = 7.35$), Table 1.

Discussion

Although the majority of the tissue mass making up renal cortex is widely held to be comprised of proximal tubule epithelial cells, cells from the thick ascending limb, distal convoluted tubule, connecting tubule, cortical collecting duct, blood vessels and glomeruli are also present to lesser extent in the cortex (Verlander, 1998). The cell-isolation procedure used slices of outer cortex to enrich the preparation for proximal tubule cells. This method yielded a population of single spherical cells that did not exhibit any obvious brush-border morphology and did not appear to retain their epithelial polarity. Solute-induced cell swelling of the proximal tubule has been observed in both amphibian and mammalian proximal tubule preparations. Such swelling is attributed to stimulation of Na^+-solute cotransport, a subsequent increase in the intracellular concentrations of Na^+ and solute, an influx of osmotically obliged water and cell swelling (Beck & Potts, 1990; Weinstein & Clausen, 1994; Mounfield & Robson, 1998). In this study, cells were examined over the size range 8.75 to 10.5 μm. All of the cells in this size range demonstrated swelling on exposure to L-alanine, indicating that these cells were originated from the proximal tubule. Further evidence supporting the proximal tubule origin of the cells used in this study is provided from micropuncture studies (Kibble et al., 2001), where in $Cftr^{tm2cam}$ mice, only 7 out of 82 (9%) superficial nephrons demonstrated visible surface distal convolutions. Additionally, out of a total of 141 whole-cell patch recordings, there were no apparent electrophysiological differences that would suggest the presence of more than one population of cells.

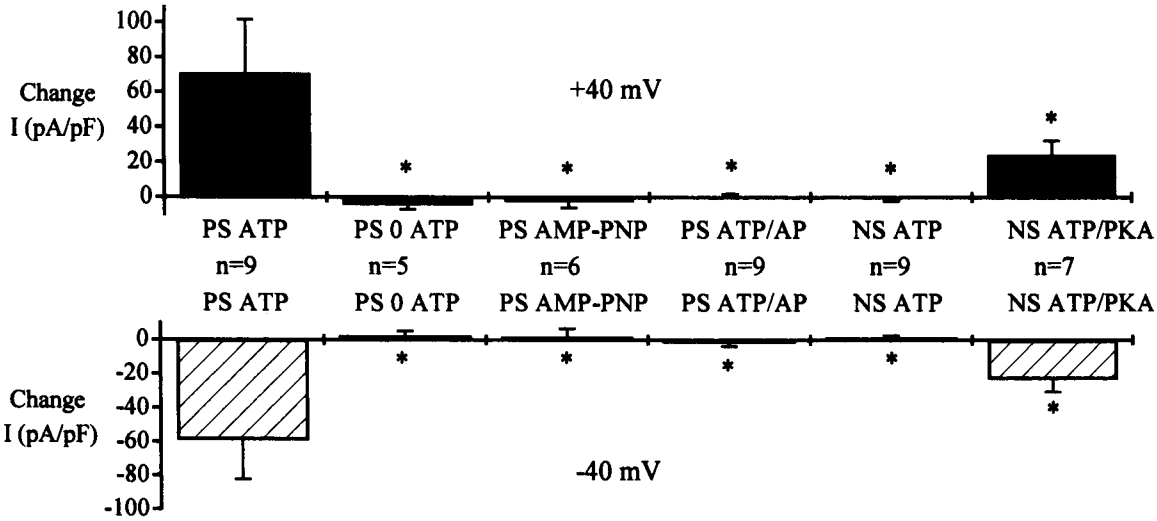

Fig. 4. Mechanism of activation of G_{NS}. Mean change in current recorded at +40 mV (*upper panel*) and −40 mV (*lower panel*). PS indicates data from cells prestimulated with dbcAMP and IBMX. NS indicates control unstimulated cells. * indicates a significant difference compared to PS cells with 5 mM ATP in the pipette (PS-ATP). $F_{5,39} = 4.46$ and $F_{5,39} = 5.10$ for the +40 and −40 mV data, respectively.

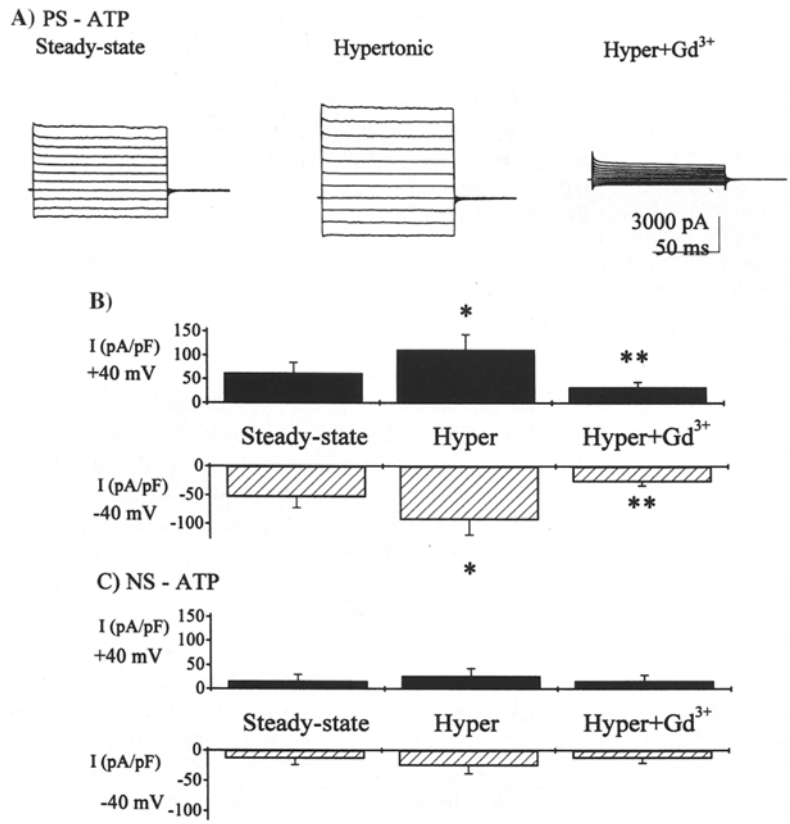

Fig. 5. Effect of hypertonic shock on whole-cell currents. (*A*) Typical whole-cell traces obtained from the same cell (prestimulated in the presence of 5 mM pipette ATP). (*B*) Mean current density data from cAMP pre-stimulated cells (PS-ATP) at +40 mV and −40 mV. * indicates a significant difference compared to steady state. ** indicates a significant difference compared to hypertonic shock. (*C*) Mean current density of unstimulated cells (NS-ATP) at +40 mV and −40 mV.

The present study demonstrates that single proximal tubule cells isolated from mouse kidney contain a nonselective conductance, designated G_{NS}. G_{NS} was activated in the presence of pipette ATP, but only when cells were exposed to a cAMP-stimulating cocktail. In cAMP-prestimulated cells in the absence of pipette ATP, activation of G_{NS} was absent. These data support the hypothesis that the activation of G_{NS} is dependent on both the presence of intracellular ATP and high levels of intracellular cAMP. This requirement for ATP is in contrast to the activation of cation channels in HT_{29} cells, smooth muscle cells and a renal proximal tubule cell line where activation was observed in the absence of pipette ATP (Koch &

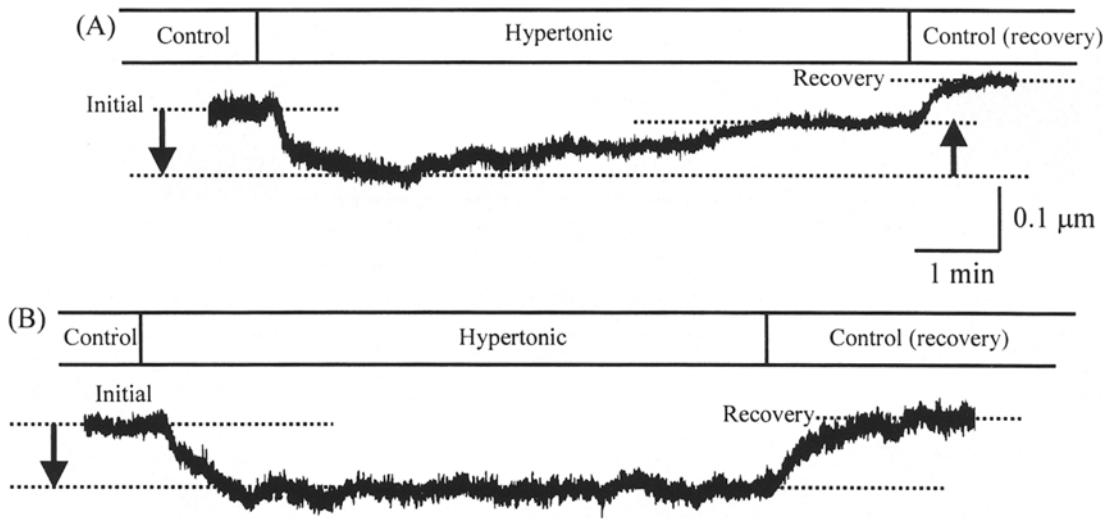

Fig. 6. Typical cell-diameter traces obtained from (*A*) a regulating cell and (*B*) a non-regulating cell. Initial: diameter in control Ringer; ↓: maximum decrease from initial diameter in response to hypertonic shock; ↑: increase to steady state during RVI.

Table 1. RVI in mouse renal proximal tubule cells

Experimental group	Regulating cells					Non-regulating cells		
	Initial (μm)	↓ (μm)	↑ (μm)	Difference (μm)	*n*	Initial (μm)	↓ (μm)	*n*
Unstimulated	10.2 ± 0.19	0.39 ± 0.07	0.45 ± 0.14	0.05 ± 0.12	7	9.56 ± 0.27	0.61 ± 0.07	9
cAMP	9.73 ± 0.22	0.21 ± 0.03	0.17 ± 0.05	−0.04 ± 0.07	7	9.76 ± 0.37	0.37 ± 0.09	5
100 μM Gd^{3+}	9.88 ± 0.17	0.31 ± 0.10	0.24 ± 0.07	−0.07 ± 0.10	6	9.51 ± 0.14	0.26 ± 0.03	7
Isolation Gd^{3+}	9.99 ± 0.10	0.29 ± 0.05	0.29 ± 0.06	0.01 ± 0.08	9	9.89 ± 0.23	0.33 ± 0.06	4

Initial: diameter in control Ringer; ↓: maximum decrease in response to hypertonic shock; ↑: increase to steady state during RVI; Difference: steady-state diameter after RVI with respect to initial level (where 0 = initial diameter, positive value = diameter greater than initial, and negative value = diameter lower than the initial level), *n* = number of cells.

Korbmacher, 1999). In addition, in the amphibian proximal tubule, mouse collecting duct and mouse proximal tubule intracellular ATP inhibits activation of nonselective conductances (Chraibi et al., 1994; Volk et al., 1995; Hurwitz et al., 2002). Nonselective conductances that require the presence of intracellular ATP have been observed in the frog proximal tubule (Robson & Hunter, 2000) and in Caco-2 cells (Nelson et al., 1996). The magnitude of the whole-cell currents associated with G_{NS} was comparable to whole-cell nonselective currents recorded in cortical collecting duct cells from rats and mice (Schlatter et al., 1997; Volk et al., 1995).

The mechanism of action of ATP requires ATP hydrolysis, as replacement of ATP with the non-hydrolyzable analogue AMP-PNP did not support activation of G_{NS}. This is consistent with the nonselective conductance in Caco-2 cells, which fails to activate when pipette ATP was replaced by a non-hydrolyzable analogue (Nelson et al., 1996). It is also similar to the nonselective conductance in M1 cells, which requires an ATP-mediated phosphorylation event for activation (Koch & Korbmacher, 2000), although this conductance is inhibited by high concentrations of ATP (Volk et al., 1995). The nonselective conductance observed in frog proximal tubule cells (Robson & Hunter, 2000) was only partially inhibited by AMP-PNP substitution. In addition, ATP-dependent activation also required a phosphorylation step, as activation was inhibited when the pipette contained ATP together with alkaline phosphatase. This phosphorylation-dependent activation of G_{NS} is consistent with the nonselective conductances observed in mouse and guinea pig pancreatic acinar cells (Suzuki & Koyama, 1996) and Caco-2 cells (Nelson et al., 1996). The mechanism of activation appears to involve a PKA-mediated phosphorylation event, as activation of G_{NS} could be observed in unstimulated cells in the presence of ATP together with the catalytic subunit of PKA. The current activated by ATP and PKA demonstrated the same properties as G_{NS}, linear, cation-selective and sensitive to Gd^{3+}, suggesting that this conductance was attributable to G_{NS}. Taken together with the requirement for activation of cAMP, these data suggest that the activation of G_{NS} occurs via a PKA-mediated

phosphorylation event. Again, this is similar to the nonselective conductances observed in pancreatic acinar cells, which are activated by PKA and require the presence of intracellular ATP (Suzuki & Koyama, 1996), although it is different from the Caco-2 nonselective conductance, which requires protein kinase C for activation (Nelson et al., 1996). The ATP concentration in rabbit proximal tubule cells has been shown to vary between 2–4 mM (Beck et al., 1991). This suggests that the concentration of ATP required for the activation of G_{NSC} falls within the physiological range and that G_{NS} could be regulated by the metabolic state of the cell.

Exposure of prestimulated cells, with ATP in the pipette, to a hypertonic bath solution resulted in an increase in the magnitude of G_{NS}. There was no significant hypertonicity-stimulated increase of whole-cell currents observed in cells that did not receive pretreatment with cAMP cocktail. One explanation for the inability of hypertonic conditions to stimulate G_{NS} without pretreatment could be that phosphorylation of a regulatory intracellular protein or the G_{NS} channel protein is required to render the conductance sensitive to hypertonicity. Another explanation could be that G_{NS} is only sensitive to hypertonicity when it is already open. Finally, the lack of stimulation of G_{NS} by hypertonicity in non-pretreated cells could be due to the osmotic shock utilized, which may not be a sufficient stimulus for activation in the absence of prestimulation. Alternatively, under these circumstances the number of active channels in the patch available for hypertonic shock-induced activation could be lower than in the prestimulated cells. Interestingly, when the hypertonic currents were expressed as a fraction of the initial level, there was no significant difference between the stimulated and unstimulated cells. The nonselective conductances identified in cultured mouse collecting duct cells (Volk et al., 1995) and Caco-2 cells (Nelson et al., 1996) were activated by hypertonic shocks of +100 and +80 mOsm/kg H_2O respectively. The current activated by the hypertonic shock was linear, did not show any voltage- or time-dependent activation and was inhibited by Gd^{3+}, properties consistent with the activation of G_{NS}.

G_{NS} demonstrated the properties of a nonselective conductance. However, G_{NS} did not demonstrate any rectification. This is in contrast to other nonselective conductances in HT_{29} cells and mouse collecting duct, which demonstrate slight outward rectification (Koch & Korbmacher, 1999; Volk et al., 1995). Like these conductances, G_{NS} did not demonstrate any voltage- or time-dependent activation. G_{NS} was inhibited in an irreversible manner by the cation-channel blocker Gd^{3+}, with a K_d of 75 μM at −80 mV. Such irreversible inhibition by Gd^{3+} has been observed in previous studies of the properties of nonselective conductances (Robson & Hunter, 2000; Filipovic & Sackin, 1991). The PKA-stimulated current also had a linear *I-V* relationship and was inhibited by Gd^{3+}. The Gd^{3+} sensitivty of G_{NS} is similar to other hypertonicity-activated conductances, which are strongly inhibited by 10 to 1000 μM Gd^{3+} (Chan & Nelson, 1992; Volk et al., 1995; Schlatter et al., 1997). G_{NS} increased the cation selectivity of whole-cell currents. On initially achieving the whole-cell configuration, whole-cell currents did not discriminate between cations and anions. After activation of G_{NS}, whole-cell current was more cation selective, although the selectivity was low, only 1.5 times more selective for cations over anions. Although the initial currents did not demonstrate a significant shift in V_{rev} on dilution of bath NaCl, three of the patches demonstrated a shift that was comparable to the shift observed after activation, suggesting that in some cells G_{NS} was already active in the patch. In the absence of the activation of G_{NS}, whole-cell currents remained nonselective. The cation:anion selectivity of the Gd^{3+}-sensitive currents (2:1) confirmed that G_{NS} was more selective for cations than anions. However, this selectivity ratio is lower than that usually reported for nonselective conductances, although it is similar to that of the shrinkage-activated cation conductance observed in Caco-2 cells (Chan & Nelson, 1992; Volk et al., 1995; Nelson et al., 1996). Like other non-selective hypertonicity-activated conductances, G_{NS} did not discriminate between Na^+ and K^+ (Chan & Nelson, 1992; Volk et al., 1995; Schlatter et al., 1997). From shifts in V_{rev}, G_{NS} did also not discriminate well between NMDG and Na^+, However, the magnitude of both the outward and inward currents carried by G_{NS} with NMGD as the main bath cation was significantly reduced compared to Na^+. This suggests that although G_{NS} does not discriminate well between NMDG and Na^+, once in the channel pore NMGD may inhibit current flow through the channel.

The hypertonicity-induced increase in G_{NS} infers that it is activated by cell-shrinkage, a property that has been suggested for a number of nonselective conductances (Chan & Nelson, 1992; Volk et al., 1995; Nelson et al., 1996). The activation of these conductances by cell shrinkage may play an important role in RVI, with activation allowing Na^+ and Cl^- to enter the cell, leading to osmotic influx of water and an increase in cell volume. Examination of the effect of a hypertonic shock on single mouse proximal tubule cells demonstrated that a sub-population was capable of RVI, with the remaining cells maintaining a reduced cell diameter in the presence of a hypertonic shock. A subdivision of cell-diameter responses to hypotonic shock and subsequent RVD has been observed previously in both mammalian and amphibian proximal tubule cells (Robson & Hunter, 1994; Millar et al., 2001). These data suggest that a similar division exists with proximal tubule

RVI. RVI was unaffected by cAMP prestimulation. It was also unaffected by the presence of 100 μM Gd^{3+}, a concentration that inhibited about 60% of G_{NS}. These data suggest that while G_{NS} is stimulated by hypertonic cell shrinkage, it does not play an important role in RVI. This is in contrast to a study in a human heptoma cell line where Gd^{3+} inhibited RVI (Wehner et al., 2002). However, these results must be approached with caution since Gd^{3+} influences a number of cellular proteins. Therefore, it is still possible that G_{NS} may actually play a role in the RVI response of mouse proximal tubule cells, but that the influence of Gd^{3+} on other transport mechanisms could be masking the effects of blocking G_{NS} on RVI.

In summary, these data provide evidence for the existence of a hypertonicity-activated nonselective conductance in single cells isolated from mouse proximal tubule, G_{NS}. The activation of G_{NS} by hypertonic shock was dependent on prestimulation of cAMP. G_{NS} was also activated by prestimulation of cAMP together with pipette ATP. Activation of G_{NS} was abolished in the presence of pipette AMP-PNP, ATP plus alkaline phosphatase or in the absence of ATP. In the unstimulated cells, G_{NS} was activated by pipette ATP together with PKA. These data support the hypothesis that G_{NS} is activated by a PKA-mediated phosphorylation event, and that such activation may occur in response to a hypertonic shock. G_{NS} does not appear to be involved in RVI, as RVI was unaffected by the presence of the G_{NS} blocker Gd^{3+}. Instead, the ATP sensitivity of G_{NS} suggests that it may be regulated by the metabolic state of the renal proximal tubule cell.

This work was supported by the National Kidney Research Fund and the Wellcome Trust.

References

Bear, C.E. 1990. A nonselective cation channel in rat liver cells is activated by membrane stretch. *Am. J. Physiol.* **258:**C421–C428

Beck, J.S., Breton, S., Mairbraul, H., Laprade, R., Giebisch, G. 1991. Relationship between sodium transport and intracellular ATP in isolated perfused rabbit proximal convoluted tubule. *Am. J. Physiol.* **261:**F634–F639

Beck, J.S., Potts, D.J. 1990. Cell swelling, co-transport activation and potassium conductance in isolated perfused rabbit kidney proximal tubules. *J. Physiol.* **425:**369–378

Chan, H.C., Nelson, D.J. 1992. Chloride-dependent cation conductance activated during cellular shrinkage. *Science* 257:669–671

Chraibi, A., Van den Abbeele, T., Guinamard, R., Teulon, J. 1994. A ubiquitous non-selective cation channel in the mouse renal tubule with variable sensitivity to calcium. *Pfluegers Arch.* **429:**90–97

Christensen, O. 1987. Mediation of cell volume regulation by calcium influx through stretch-activated channels. *Nature* **330:**66–68

Douglas, I.J., Brown, P.D. 1996. Regulatory volume increase in rat lacrimal gland acinar cells. *J. Membrane Biol.* **150:**209–217

Filipovic, D., Sackin, H. 1991. A calcium-permeable stretch-activated cation channel in renal proximal tubule. *Am. J. Physiol.* **260:**F119–F129

Gustin, M.C., Zhou, X.L., Martinac, B., Kung, C. 1988. A mechanosensitive ion channel in the yeast plasma membrane. *Science* **242:**762–765

Hamill, O.P., Marty, A., Neher, E., Sakmann, B., Sigworth, F.J. 1981. Improved patch clamp techniques for high resolution current recording from cells and cell free membrane patches. *Pfluegers Arch.* **391:** 85–100

Hoyer, J., Goegelein, H. 1991. Sodium-alanine cotransport in renal proximal tubule cells investigated by whole-cell current recording. *J. Gen. Physiol.* **97:**1073–1094

Hurwitz, C.G., Hu, V.Y., Segal, A.S. 2002. A mechanogated nonselective cation channel in proximal tubule that is ATP sensitive. *Am. J. Physiol.* **283:**F93–F104

Kibble, J.D., Balloch, K.J.D., Neal, A.M., Hill, C., White, S.J., Robson, L., Green, R., Taylor, C.J. 2001. Renal proximal tubule function is preserved in *Cftr*^{tm2cam} delta F508 cystic fibrosis mice. *J. Physiol.* **532:**449–457

Koch, J.-P., Korbmacher, C. 1999. Osmotic shrinkage activates nonselective cation (NSC) channels in various cell types. *J. Membrane Biol.* **168:**131–139

Koch, J.-P., Korbmacher, C. 2000. Mechanism of shrinkage activation of nonselective cation channels in M-1 mouse cortical collecting duct cells. *J. Membrane Biol.* **177:**231–242

Lopes, A.G., Guggino, W.B. 1987. Volume regulation in the early proximal tubule of the *Necturus* kidney. *J. Membrane Biol.* **97:**117–125

Miley, H.E., Holden, D., Grint, R., Best, L., Brown, P.D. 1998. Regulatory volume increase in rat pancreatic beta cells. *Pfluegers Arch.* **435:**227–230

Millar, I.D., White, S.J., Kibble, J.D., Robson, L. 2001. Regulatory volume decrease is defective in renal proximal tubule cells isolated from IsK knockout mice. *J. Physiol.* **531P:**123P

Mounfield, P.R., Robson, L. 1998. The role of Ca^{2+} in volume regulation induced by Na^{+}-coupled alanine uptake in single proximal tubule cells isolated from frog kidney. *J. Physiol.* **510:**145–153

Nelson, D.J., Tien, X.-Y., Xie, W., Brasitus, T.A., Kaetzel, M.A., Dedman, J.R. 1996. Shrinkage activates a nonselective conductance: involvement of a Walker motif and PKC. *Am. J. Physiol.* **270:**C179–C191

Robson, L., Hunter, M. 1994. Volume regulatory responses in frog isolated proximal cells. *Pfluegers Arch.* **428:**60–68

Robson, L., Hunter, M. 2000. An intracellular ATP-activated, calcium-permeable conductance on the basolateral membrane of single renal proximal tubule cells isolated from *Rana temporaria*. *J. Physiol.* **523:**301–311

Sachs, F. 1987. Baroreceptor mechanisms at the cellular level. *Fed. Proc.* **46:**12–16

Schlatter, E., Ankorina-Stark, I., Cermak, R., Haxelmans, S., Kleta, R., Hirsch, J.R. 1997. Cell shrinkage activates a cation conductance in principal cells of rat cortical collecting duct. *Cell Physiol. Biochem.* **7:**321–332

Suzuki, K., Koyama, I. 1996. Comparison of non-selective cation channels by protein kinase-A in guinea-pig and mouse pancreatic acinar cells. *Jap. J. Physiol.* **46:**43–52

Takenaka, T., Suzuki, H., Okada, H., Hayashi, K., Kanno, Y., Saruta, T. 1998. Mechanosensitive cation channels mediate afferent arteriolar myogenic constriction in the isolated rat kidney. *J. Physiol.* **511:**245–253

Verlander, J.W. 1998. Normal renal function and alterations of renal function in states of nephrotoxicity. *Toxicol. Pathol.* **26:**1–17

Volk, T., Frömter, E., Korbmacher, C. 1995. Hypertonicity activates nonselective cation channels in mouse cortical collecting duct cells. *Proc. Natl. Acad. Sci. USA* **92:**8478–8482

Waldegger, S., Steuer, S., Risler, T., Heidland, A., Capasso, G., Massry, S., Lang, F. 1998. Mechanisms and clinical significance of cell volume regulation. *Nephrol. Dial. Transplant* **13:** 867–874

Wehner, F., Lawonn, P., Tinel, H. 2002. Ionic mechanisms of regulatory volume increase (RVI) in the human hepatoma cell-line HepG2. *Pfluegers Arch* **443:**790

Wehner, F., Tinel, H. 1998. Role of Na^+ conductance, Na^+-H^+ exchange, and Na^+-K^+-$2Cl^-$ symport in the regulatory volume increase of rat hepatocytes. *J. Physiol.* **506:**127–142

Weinstein, S.W., Clausen, C. 1994. Adaptive responses to Na^+-coupled solute transport and osmotic cell swelling in salamander proximal tubule. *Am. J. Physiol.* **267:**F479–F488

Welling, P.A., O'Neil, R.G. 1990. Cell swelling activates basolateral membrane Cl and K conductances in rabbit proximal tubule. *Am. J. Physiol.* **258:**F951–F962

Wellner, M.-C., Isenberg, G. 1993. Properties of stretch-activated channels in myocytes from the guinea-pig urinary bladder. *J. Physiol.* **466:**213–227

Wison, G.F., Magoski, N.S., Kaczmarek, L.K. 1998. Modulation of a calcium-sensitive nonspecific cation channel by closely associated protein kinase and phosphatase activities. *Proc. Natl. Acad. Sci. USA* **95:**10938–10943